รายงานวิจัยฉบับสมบูรณ์

โครงการการศึกษาเชิงโครงสร้างของสารประกอบ $Bi(Mg_{1/2}Ti_{1/2})O_3$ จาก Density functional theory

โดย

ดร. มัลลิกา ซื่อวัฒนะ และ คณะ

ภาควิชาฟิสิกส์ คณะวิทยาศาสตร์ มหาวิทยาลัยมหิดล

กันยายน 2551

สัญญาเลขที่ MRG5280199

รายงานวิจัยฉบับสมบูรณ์

โครงการการศึกษาเชิงโครงสร้างของสารประกอบ $Bi(Mg_{½}Ti_{½})O_3$ จาก Density functional theory

ดร. มัลลิกา ซื่อวัฒนะ และ คณะ
สังกัด
ภาควิชาฟิสิกส์ คณะวิทยาศาสตร์ มหาวิทยาลัยมหิดล

สนับสนุนโดยสำนักงานคณะกรรมการการอุดมศึกษา
และสำนักงานกองทุนสนับสนุนการวิจัย

Abstract

Project Code: MRG5280199

Project Title: Crystal structure study of $Bi(Mg_{1/2}Ti_{1/2})O_3$ by density functional theory

Investigator: Dr. Malliga Suewattana E-mail Address : smsw@mahidol.ac.th

Department of Physics, Faculty of Science, Mahidol University, Bangkok

Dr. David J Singh E-mail Address : singhdj@ornl.gov

Material Science and Technology division, Oak Ridge National Laboratory, Oak Ridge, TN USA

Prof. Sukit Limpijumnong E-mail Address : konesarn@gmail.com

School of Physics, Suranaree University of Technology and National Synchrotron Research center, Nakhon Ratchasima 30000

Project Period: 15 March 2008 to 15 September 2011

Piezoelectrics materials have been in use commercially for several decades, but it has been only in the past decade that many developments and the rapid growth have shown. This is in part connected to large number of modern technological applications such as multilayer capacitors, actuators, motors, micropositioning systems. For a lengthy period of time, Pb-based piezoelectric such as $Pb(Zr_{1-x}Ti_x)O_3$ (PZT) has dominated due to its exceptional piezoelectric response at the composition close to the morphotropic phase boundary (MPB). A large number of applications of PZT yield an every greater amount of Pb into the environment. As a consequence, a large number of efforts have been conducted over a wide area of researchs in search for materials which could be used to replace Pb-based piezoelectric. Among many promising candidates, Bi-based compounds have stimulated great interest due to its various similarities in chemistry as Pb which results in an improvement in piezoelectric properties. Here we focus on a mixed B-site Bi compounds, $Bi(Mg_{1/2}Ti_{1/2})O_3$ (BMT) which has been shown as being one of the promising candidates to be lead free ferroelectric materials. BMT has reported as having the same structure as the antiferroelectric $PbZrO_3$. However, results from experiment have shown the BMT X-ray

refinement cannot distinguish the structure between Pbam and Pnnm but the octahedral tilting analysis suggested the Pbam being the spacegroup BMT. This stimulated our interest in investigating and verifying the structure of BMT by mean of the theoretical tool, density functional theory.

We used first principles supercell calculations to reexamine the atomic coordinates of crystalline $Bi(Mg_{1/2}Ti_{1/2})O_3$ from the X-ray diffraction for Pbam and Pnnm supercells. The calculations show the difference in atomic positions up to 0.5 angstrom in which the most deviation appears in O atom for Pbam supercell and metal cations in Pnnm supercell. The features of the octahedral rotation/tilting agree well with the X-ray results. The calculated structures are further analyzed with pair distribution function showing that the most significant changes are in the local Bi coordinate for Pnnm and O for Pbam. Calculated electric field gradient are also reported. The results are discussed in relation to the structure of $PbZrO_3$.

Keywords : ferroelectrics, first principles calculations, bismuth magnesium titanates, lead-free

บทคัดย่อ

รหัสโครงการ: MRG5280199

ชื่อโครงการ: การศึกษาเชิงโครงสร้างของสารประกอบ $Bi(Mg_{½}Ti½)O_3$ จาก density functional theory

ชื่อนักวิจัย ดร. มัลลิกา ซื่อวัฒนะ E-mail Address : smsw@mahidol.ac.th
ภาควิชาฟิสิกส์ คณะวิทยาศาสตร์ มหาวิทยาลัยมหิดล กรุงเทพฯ
Dr. David J Singh E-mail Address : singhdj@ornl.gov
Material Science and Technology division, Oak Ridge National Laboratory,
Oak Ridge, TN USA
ศาสตราจารย์ ชูกิจ ลิมปิจำนงค์ E-mail Address : konesarn@gmail.com
สาขาวิชาฟิสิกส์ สำนักวิชาวิทยาศาสตร์ มหาวิทยาลัยเทคโนโลยีสุรนารี
นครราชสีมา 30000

ระยะเวลาโครงการ: 15 March 2008 to 15 September 2011

สารประกอบพิโซอิเล็กตริกได้มีการประยุกต์ใช้มาเป็นเวลาหลายทศวรรษ แต่มีแค่ในช่วงเวลาสิบปีที่ผ่านมาเท่านั้นที่การพัฒนาทั้งในด้านการวิจัยและการนำไปใช้ได้เพิ่มขึ้นอย่างรวดเร็ว เหตุผลอย่างหนึ่งก็คือมีการใช้สารประกอบเหล่านี้ในอุตสาหกรรมมากขึ้น ดังนั้นจึงมีความจำเป็นที่ต้องผลิตสารประกอบพิโซอิเล็กตริกให้มีประสิทธิภาพมากขึ้นเช่นกัน โดยทั่วไปสำหรับการใช้สารประกอบพิโซอิเล็กตริก สารประกอบที่มีส่วนผสมของตะกั่ว โดยเฉพาะ $Pb(Zr_{1-x}Ti_x)O_3$ (PZT) จะมีการใช้อย่างแพร่หลายเนื่องจากสารประกอบชนิดนี้มีคุณสมบัติทางพิโซอิเล็กตริกและเฟอร์โรอิเล็กตริกที่ดีกว่าสารตัวอื่นๆมาก โดยเฉพาะที่สัดส่วนของ Zr และ Ti อยู่ที่ตำแหน่งที่เรียกว่า morphotropic phase boundary (MPB) ซึ่งเป็นอัตราส่วนประมาณ x=0.48 โดยคุณสมบัติทางพิโซอิเล็กตริก จะมีค่ามากที่สุด การนำเอาสารประกอบ PZT ไปใช้ในอุตสาหกรรมทำให้มีการปล่อยสารตะกั่วลงสู่สิ่งแวดล้อมเป็นจำนวนมากซึ่งเป็นปัญหาทางมลพิษ ดังนั้นจึงมีความร่วมมือจากกลุ่มวิจัยหลายๆกลุ่มเพื่อจะหาสารประกอบไร้ตะกั่วที่มีคุณสมบัติใกล้เคียง PZT หนึ่งในสารประกอบเหล่านั้นคือสารประกอบที่มี Bi ปนอยู่ เนื่องจาก Bi และ Pb มีการจัดเรียงตัวของอิเล็กตรอนวงนอกคล้ายๆกัน ทำให้ สารประกอบของBi มีแนวโน้มที่จะมีคุณสมบัติทางพิโซอิเล็กตริกใกล้เคียง PZT

สารประกอบที่เราสนใจคือ $Bi(Mg_{1/2}Ti_{1/2})O_3$ (BMT) ซึ่งเป็นสารประกอบ perovskite ที่มี B-cations ประกอบด้วยอะตอมสองชนิดคือ Mg และ Ti และเป็นตัวเลือกที่น่าสนใจสำหรับสารประกอบเฟอร์โรอิเล็กตริกไร้สารตะกั่ว ในผลของการทดลองทางปฏิบัติพบว่าBMT มีโครงสร้างใกล้เคียงกับสารประกอบ แอนติเฟอร์โรอิเล็กตริก $PbZrO_3$ เนื่องจากผลของ X-ray refinement ไม่สามารถแยกโครงสร้างของ BMT ได้ว่าเป็น Pbam หรือ Pnnm โดยที่ Pnnm เป็นโครงสร้างของ $PbZrO_3$ ดังนั้นทางกลุ่มวิจัยต้องการศึกษาและชี้เฉพาะโครงสร้างของ BMT โดยการใช้ density functional theory

การวิจัยนี้ศึกษาโครงสร้างของสารประกอบ $Bi(Mg_{1/2}Ti_{1/2})O_3$ โดยใช้การคำนวนแบบ first principles supercells ซึ่งเน้นโครงสร้างที่ได้จากการวิจัยเชิงปฏิบัติสองชนิดคือ Pbam และ Pnnms supercells ผลการวิจัยพบว่า ตำแหน่งอะตอมของแคทอิออนระหว่างผลการวิจัยทางปฏิบัติและการคำนวนบิดเบือนแตกต่างกันประมาณ 0.5 อังสตรอม โดยที่การเปลี่ยนแปลงพบมากที่สุดคืออะตอมของออกซิเจนใน Pbam supercell และ แคทอิออนของ Pnnm supercell สำหรับการหมุนและการบิดเบี้ยวของกรงออกซิเจนแปดเหลี่ยมของทั้งสองโครงสร้างสอดคล้องกับผลของการวิจัยเชิงปฏิบัติ นอกจากนี้ผลของโครงสร้างที่ได้ยังได้ถูกนำไปวิเคราะห์โดยใช้ pair distribution function ปรากฏว่าการบิดเบือนของโครงสร้างโดยรวมแล้วพบอยู่ที่อะตอมของ Bi ของ Pnnm ซึ่งเป็นอะตอมที่รับผิดชอบต่อการเป็นเฟอโรอิเล็กตริกของสารประกอบนี้ และออกซิเจนของ Pbam นอกเหนือจากการวิเคราะห์ทางโครงสร้างแล้วมีการรายงานค่าของ electric field gradient ซึ่งเป็นปัจจัยชี้บอกของการบิดเบี้ยวของตำแหน่งนิวเคลียร์ของสารประกอบ ผลการวิจัยทั้งหมดถูกวิเคราะห์และเปรียบเทียบกับคุณสมบัติของสารประกอบ $PbZrO_3$ ที่มีคุณสมบัติเป็นแอนติเฟอร์โรอิเล็กตริก แต่เชื่อว่ามีโครงสร้างเดียวกันสารประกอบที่สนใจ

คำหลัก: เฟอร์โรอิเล็กตริก, first principles calculations, บิสมัทแมกนีเซียมไททาเนต, สารประกอบไร้ตะกั่ว

กิติกรรมประกาศ

งานวิจัยนี้ สำเร็จได้ด้วยดี โดยได้รับการสนับสนุนเงินทุน และการหนุนเสริมด้านต่างๆจาก สำนักงานคณะกรรมการการอุดมศึกษา (สกอ) สำนักงานกองทุนสนับสนุนการวิจัย (สกว) ภาควิชาฟิสิกส์ คณะวิทยาศาสตร์ บัณฑิตวิทยาลัย มหาวิทยาลัยมหิดล Department of Physics College of William and Mary, Virginia USA และ Oak Ridge National Laboratory Tennessee USA

คณะผู้วิจัยของกราบขอบพระคุณ ผศ. ศรีสุดา วรามิตร หัวหน้าภาควิชาฟิสิกส์ คณะวิทยาศาสตร์ มหาวิทยาลัยมหิดล และ ศ. ศกรณ์ มงคลสุข คณะบดี คณะวิทยาศาสตร์ มหาวิทยาลัยมหิดล ที่ให้การสนับสนุน และอนุญาตให้ผู้วิจัยลาวิจัยเพื่อดำเนินการร่วมกับกลุ่มวิจัยที่ประเทศสหรัฐอเมริกา

การวิจัยนี้ได้รับความอนุเคราะห์ใช้ทรัพยากรการคำนวนจาก Snowflake cluster (ครุภัณฑ์ของทุนพัฒนาศักยภาพในการทำงานวิจัยของอาจารย์รุ่นใหม่ รหัสโครงการ: MRG5280199) High performance computer cluster ของ condensed matter theory group สาขาวิชาฟิสิกส์ สำนักวิทยาศาสตร์ มหาวิทยาลัยเทคโนโลยีสุรนารี High performance computer cluster (mu-hpc) ของ คณะวิทยาศาสตร์ มหาวิทยาลัยมหิดล High performance computer cluster ของ center of piezoelectric by design Newport News, Virginia USA

ขอขอบคุณคณะวิจัยทุกท่าน คณาจารย์ภาควิชาฟิสิกส์ คณะวิทยาศาสตร์ มหาวิทยาลัยมหิดล Condensed matter theory group College of William and Mary Condensed matter theory group สาขาวิชาฟิสิกส์ สำนักวิทยาศาสตร์ มหาวิทยาลัยเทคโนโลยีสุรนารี เจ้าหน้าที่ธุรการ ภาควิชาฟิสิกส์ คณะวิทยาศาสตร์ มหาวิทยาลัยมหิดล ที่มีส่วนร่วมในการทำงานวิจัยครั้งนี้ให้ประสบความสำเร็จ

มัลลิกา ซื่อวัฒนะ

กันยายน 2554

Table of Contents

List of Tables and Figures

Chapter 1: Introduction

Piezoelectric and ferroelectric crystals are known for their important technological applications such as high-permittivity dielectrics, piezoelectric sensors, transducers, and mechanical actuators [1]. The sensors based on the piezoelectric effect transform mechanical signals into electrical signals while the piezoelectric actuators transform electrical signals into mechanical signals. Ferroelectric materials are a special class of piezoelectrics, which exhibit, a large piezoelectric response. Besides piezoelectric applications, optical, thermal and electrical properties of ferroelectrics are exploited in a large number of devices and components, including capacitors and nonvolatile memories where electrical voltage is used to displace electrical charge. Recently, single crystal relaxor perovskite such as $Pb(Zn_{1/3}Nb_{2/3})O_3$-$PbTiO_3$ (PZN-PT) and $Pb(Mg_{1/3}Nb_{2/3})O_3$-$PbTiO_3$ (PMN-PT) were synthesized and found to exhibit ultrahigh strain and very large piezoelectric constants [1-3]. The structure of alloys like PMN-PT can be viewed as a perovskite ABO_3 framework (a cubic lattice for the ideal perovskite crystal), with Pb ions on the A-site and a solid solution of (Mg^{2+}, Nb^{5+}, Ti^{4+}) ions on the B-sites. Of course this is an idealized picture, neglecting vacancies, impurities, local structural distortions and partial chemical ordering on the B-sites. The ideal cubic ABO_3 perovskite can be viewed as a perfectly cubic box with the A atoms are at the cube corner, the O atoms are at the face centers and the B atom is at the cube center which forms an octahedron with the O sites. The origin of the ferroelectric behavior is unclear for these perovskite materials, however, there is an understanding of the similar, but chemically different, perovskites should display very different ferroelectric behaviors. Ferroelectricity is off great sensitivity to the chemical composition, defect, pressure due to the delicate balance between three factors as discussed by R. Cohen [4] those are the long range Coulomb forces which favors the ferroelectric state, the short-range repulsion which favors the paraelectric cubic structure and the hybridization between metal d orbital and oxygen p orbital.

For the past few decades, ceramics based on the Pb-based perovskite systems have come to dominate the market of ferroelectric and piezoelectric ceramics. Example of such class of

materials include isoelectronic solid solution like $Pb(Zr_{1-x}Ti_x)O_3$ (PZT), non-isoelectronic B-site solid solutions $Pb(BB'B'')O_3$, with B-site cations from group II, IV and V often exhibits compositionally – dependent B-site chemical ordering [5-9]. These classes of materials display the partial B-site chemical ordering which is a common feature of the high-piezoelectric solid solutions in addition to the chemistry of the lone pair of Pb cations, especially PZT which is one of the well-known relaxors exhibiting high electromechanical response. Relaxor behavior results from either frustration or compositionally induced disorder [10]. The latter type of disorder and related random fields are believed to be responsible for the relaxor properties of the most relaxor, the mixed ABO_3 perovskite oxides. Relaxor is viewed as the materials with a broad, frequency-dependent peak in the susceptibility, and are characterized by very small remanent polarization and the absence of macroscopic phase change at the transition temperature. The highest PZT piezoelectric response is found for compositions in the vicinity of the morphotropic phase boundary (MPB) [6-8]. In the search for better fundamental understanding of these complex systems and for better technological properties, many Pb-based solid solutions have been investigated [3-9]. With these in mind, there have been numerous efforts to understand the mechanism of their exceptional ferroelectric properties, local structures and the origin of their perplexing phase diagram [1, 5-9]. In recent years, there have been an increasing in regulation to remove toxic materials as lead from commercial products. This has steered the research interest toward the reduced Pb and Pb-free materials instead of the counterparts. Some of the possibilities are materials based on well-known perovskite ferroelectric oxides in which A- and B-cations are substituted for different elements, such as $BaTiO_3$, and $KNbO_3$ [11-18]. In the search for materials with comparable electromechanical properties and higher transition temperature has been difficult. For instance, the host compound $BaTiO_3$ possesses low Curie temperature causing $Ba(TiZr)O_3$ to have low T_c as well [19]. Among many substitutes for the lead-based materials, Bi-based ferroelectrics are under intense investigations due to their high T_c and comparable piezoelectricity to lead-based compounds [3,20-22]. Owing to the similarity of the electronic configuration of Bi^{3+} and Pb^{2+} shell structures in which their lone pair electron configurations could enhance the polarization and ferroelectricity. In addition, their small cation size as a role of the perovskite A-cation categorize these compounds as

being the t<1 ferroelectrics where t is the Goldschmidt tolerance factor ($t = \frac{R_A + R_o}{\sqrt{2}(R_B + R_O)}$ when R_O, R_a and R_B are atomic radii for O, A-cation and B-cation respectively). This factor often used to predict the stability of the perovskite structures. A perovskite structure is stable only if the tolerance factor is in the range $0.9 < t < 1.1$ (for example, materials with a tolerance factor lower than 0.9 or higher than 1.1 typically makes the perovskite structure unstable due to a mismatch between preferred A-O and B-O bond lengths). It follows from the similarity in the electronic structures and the lower tolerance factor, that the Bi-based compound could find a light in having comparable if not better piezoelectric and ferroelectric properties than that of the Pb-based perovskites.

Taking into consideration of the abovementioned factors, a number of compounds of the $Bi(B',B'')O_3$ types have been investigated over a vast array of criterions such as relationship between compound compositions and transition temperature [23], polarizability [24,25] and distortion of the crystal lattice [26-28]. The $Bi(Mg_{1/2}Ti_{1/2})O_3$-$PbTiO_3$ (BMT-PT) have shown to be significant to be used in the high temperature applications [29-38] because it establishes relatively high Curie temperature nearly 450°C. [39] It was mentioned by Suchomel and coworker [3] (and reference therein) that the PT-based compounds Curie temperature are related to the tolerance factor, composition of end members and crystal structure [36]. This produces the opportunity for the structural investigation in the ab initio level.

It is significant to have detail structural investigation on the end member of this compound. BMT is established using x-ray refinement by Khalyavin [27] to have orthorhombic space group Pnnm and is a structural analogy to the antiferroelectric $PbZrO_3$. Detail works show that the result of the diffraction pattern revealed either Pnnm or Pbam (with the latter being the space group of $PbZrO_3$ [40-43] but with the consideration of the octahedral rotation and A-cation shifting configuration the Pnnm is more suitable being BMT space group.

First-principles calculations have allowed great understanding of the system specific interactions that produce ferroelectricity and the dependence of these interactions [4]. There have been numerous successful studies explaining ferroelectric effect and predictions of material properties [43-44]. The purpose of this paper is to verify the structures of $Bi(Mg_{1/2}Ti_{1/2})O_3$, and to study the ferroelectric behaviors of BMT as well as to compare the result with PbZrO3. We used density-functional supercell calculations for BMT with the refined structures as obtained by

Khalyavin et. al. [27] as our starting structures in which the two investigated supercells are Pnnm and Pbam. Structural relaxation of the internal atomic positions was performed. Our results indicated that refined structures are metastable with the atomic force in the factor of 0.06 Ry. There are discrepancies between relaxed structures to refined structures around 0.5 anstrom. However, the trends in A-cation displacement and octahedral rotation are consistent with the experimental observation.

Chapter 2: Theoretical and Computation Details

2.1 Many-body Schrodinger equation

Properties of materials are governed by the interactions between the constituting electrons and nuclei which can be determined by the many-body Schrödinger equations such that the Hamiltonian is given by the summation of the kinetic energy of ions and electrons, the ion-electron, electron-electron and ion-ion potential energy. According to the Born-Oppenheimer approximation, the system can be described only by the motion of electrons and disregard the kinetic energy of ions. The Hamiltonian can now be simplified as only terms consisting electron kinetic energy and electron-electron and ion-electron potential energy. The major difficulty in solving the abovementioned equation is that the electron-electron interaction energy could not be simply expressed as a sum of isolated single-particle energies. Consequently, the correlation interaction of electrons cannot be written as a product of isolated electron wave function. Hence, the method makes use of two theorems proposing by Hohenberg and Kohn [47-48] in which the ground state properties of many-body interacting electron system are uniquely defined by the ground state electron density and the expectation value of energy is written as a functional of electron density, such that this functional reaches their minimum at the ground state density. As proposed by Kohn and Sham [49], the many-body electron system can be replaced by an auxiliary system of non-interacting particles as long as the ground state density of the auxiliary system is identical to the ground state density of many-body electrons.

Now the energy as functional of energy is the combination of terms; the Hartree energy due to the Coulomb repulsion between particles, the kinetic terms and the last term that include all the many-body effects of exchange and correlation. This last term is not known explicitly yet as a function of the electron density and it is needed to be approximated. The two most common approximations used for the exchange-correlation term is the local density approximation (LDA) and generalized gradient approximation (GGA) [48]. The basic idea of the two approximations are

such that the LDA assumes the exchange-correlation energy density at each space point *r* is assumed to be the same as energy density in the homogeneous electron gas with the same particle density. In contrast with the GGA which is the extension of LDA assuming that the exchange-correlation energy not only depends on the density but also on the magnitude of its gradient. Both approximations have different advantages over various systems. For example, GGA provides better agreement with experiment over LDAs in many cases especially in predicting the binding energy for many finite systems like molecules and surfaces, etc. However, both of them have problems to describe systems with localized d and f electrons such as transition metal compound and rare earth elements compounds.

2.2 The LAPW method

Among the most accurate schemes for solving the Kohn-Sham equations is the full-potential linearized-augmented plane wave (LAPW) method with local orbital extension [46]. In the LAPW method a basis set is introduced that is especially adapted to the problem by dividing the unit cell into two areas: the non-overlapping atomic spheres which centered at the atomic sites and the interstitial region as shown in Figure I. In these two regions different basis sets are being used. Inside atomic sphere of radius R, a linear combination of radial functions times spherical harmonic functions are used while a planewave expansion is used in the interstitial region. Each planewave is augmented by an atomic like function in every atomic sphere. The solutions to the Kohn-Sham equations are expanded in this combined basis set of LAPW's according to the linear variation method.

Figure I: Partitioning of the unit cell into atomic sphere and an interstitial region.

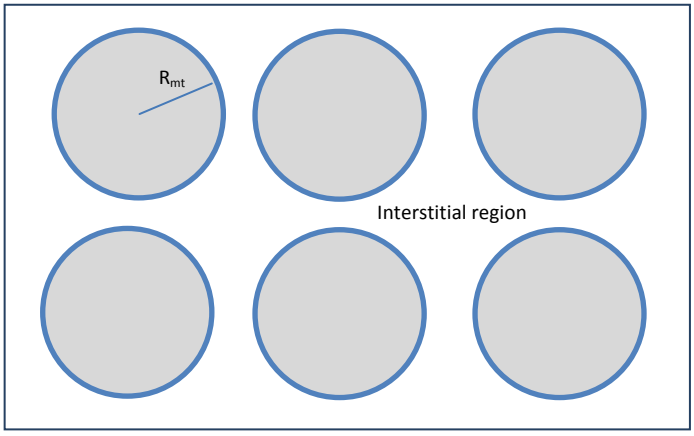

2.3 Computation details

All calculations were performed with the local density approximation (LDA) using the first-principles all-electron LAPW with local orbital method to treat the cation semicore states and to relax linearization errors [46]. Local orbitals were associated with the Bi 4s, 4p, Ti 3s, 3p, Mg 2s 2p and O 2s, 2p states. The potential and charge density has no-shape approximation. Core-electron states were calculated with a fully relativistic atomic like approximation using the self-consistent crystal potential while the valence states were treated scalar relativistically. The LAPW basis functions, charge density, and potential are all described by a dual representation. Within muffin tin spheres that are centered on the nuclear positions, these functions are represented by atomic harmonic functions. In the interstitial region between the spheres, all functions are represented by plane wave expansion. Muffin-tin sphere radii of 2.05, 1.85, 1.85, and 1.50 a.u. were used for the Bi, Ti, Mg and O ions respectively. For all systems, a well-converged $R_{MT}K_{max}=7$ is used yielding more than 12000 LAPW functions, and Monkhorst-Pack special k points were used to sample the Brillouin zone with a 4x4x4 mesh. The lattice parameters were held fixed at their experimental values a=11.3207 angstrom, b=5.6433 angstrom, c=7.8314 angstrom and a=11.3196 angstrom, b=5.6423 angstrom, c=7.8314 angstorm for Pnnm and Pbam supercells respectively and both are characterized by the $\sqrt{2}a \times \sqrt{2}b \times 2c$ unit cell . We used the subgroup of Pnnm and Pbam yielding ten inequivalent atomic positions in contrast with the eight atomic positions from the experiment. The starting positions from those of the X-ray refinement were relaxed until the interatomic force less than 0.001 Ry/a_0. The relaxed structures were analyzed with pair distribution function (PDF) and the electric field gradients of all constituents atoms were found for both structures.

Chapter 3 Results

3.1 Structural Optimization

The first procedure of our study is to obtain the ground state relaxed geometry of the solid solution $Bi(Mg_{1/2}Ti_{1/2})O_3$ under the consideration of the root mean square force of all atoms. The two systems of interest are BMT 2 formula units with Pnnm and Pbam supercells. We started with the experimental structures imposing with the sub space group listed on Table I and II respectively. The systems were perturbed by some small amount of displacement about the high symmetry positions. Then the calculations of self-consistent field were performed such that the geometries of the solid solution aim to return to equilibrium when the root mean square force reach the tolerance factor of 0.001 Ry/a_0 that was also our terminating criterion. It is important to note that in the experimental structure the Pbam and Pnnm space group were used and given the position of Mg and Ti as the same position as of the identically symmetric site of the two atoms. However, this is unpractical in the calculation point of view. We imposed the subgroup (listed in the third column of Table I and II) of Pnnm and Pbam to obtain the identical position as the experimental data. As a result, the calculations were performed on the system of ten atoms as opposed of nine atoms in the experimental data.

Table I: General positions of the Pbam group and subgroup. The transformation matrices of the group are listed in column 2 corresponding to the general position in the first column. Column 3 denotes the transformation matrices used in the calculations.

General positions		Subgroup
x, y, z	$\begin{pmatrix} 1 & 0 & 0 & 0 \\ 0 & 1 & 0 & 0 \\ 0 & 0 & 1 & 0 \end{pmatrix}$	$\begin{pmatrix} 1 & 0 & 0 & 0 \\ 0 & 1 & 0 & 0 \\ 0 & 0 & 1 & 0 \end{pmatrix}$
$-x, -y, z$	$\begin{pmatrix} -1 & 0 & 0 & 0 \\ 0 & -1 & 0 & 0 \\ 0 & 0 & 1 & 0 \end{pmatrix}$	–
$-x+\frac{1}{2}, y+\frac{1}{2}, -z$		

	$\begin{pmatrix} -1 & 0 & 0 & \frac{1}{2} \\ 0 & 1 & 0 & \frac{1}{2} \\ 0 & 0 & -1 & \frac{1}{2} \\ & & & 0 \end{pmatrix}$	$\begin{pmatrix} -1 & 0 & 0 & \frac{1}{2} \\ 0 & 1 & 0 & \frac{1}{2} \\ 0 & 0 & -1 & \frac{1}{2} \\ & & & 0 \end{pmatrix}$
$x+\frac{1}{2},-y+\frac{1}{2},-z$	$\begin{pmatrix} 1 & 0 & 0 & \frac{1}{2} \\ 0 & -1 & 0 & \frac{1}{2} \\ 0 & 0 & -1 & \frac{1}{2} \\ & & & 0 \end{pmatrix}$	–
$-x,-y,-z$	$\begin{pmatrix} -1 & 0 & 0 & 0 \\ 0 & -1 & 0 & 0 \\ 0 & 0 & -1 & 0 \end{pmatrix}$	$\begin{pmatrix} -1 & 0 & 0 & 0 \\ 0 & -1 & 0 & 0 \\ 0 & 0 & -1 & 0 \end{pmatrix}$
$x,y,-z$	$\begin{pmatrix} 1 & 0 & 0 & 0 \\ 0 & 1 & 0 & 0 \\ 0 & 0 & -1 & 0 \end{pmatrix}$	–
$x+\frac{1}{2},-y+\frac{1}{2},z$	$\begin{pmatrix} 1 & 0 & 0 & \frac{1}{2} \\ 0 & -1 & 0 & \frac{1}{2} \\ 0 & 0 & 1 & \frac{1}{2} \\ & & & 0 \end{pmatrix}$	$\begin{pmatrix} 1 & 0 & 0 & \frac{1}{2} \\ 0 & -1 & 0 & \frac{1}{2} \\ 0 & 0 & 1 & \frac{1}{2} \\ & & & 0 \end{pmatrix}$
$-x+\frac{1}{2},y+\frac{1}{2},-z$	$\begin{pmatrix} -1 & 0 & 0 & \frac{1}{2} \\ 0 & 1 & 0 & \frac{1}{2} \\ 0 & 0 & 1 & \frac{1}{2} \\ & & & 0 \end{pmatrix}$	–

Table II: General positions of the Pnnm group and subgroup. The transformation matrices of the group are listed in column 2 corresponding to the general position in the first column. Column 3 denotes the transformation matrices used in the calculations.

General positions		Subgroup
x,y,z		

	$\begin{pmatrix} 1 & 0 & 0 & 0 \\ 0 & 1 & 0 & 0 \\ 0 & 0 & 1 & 0 \end{pmatrix}$	$\begin{pmatrix} 1 & 0 & 0 & 0 \\ 0 & 1 & 0 & 0 \\ 0 & 0 & 1 & 0 \end{pmatrix}$
$-x,-y,z$	$\begin{pmatrix} -1 & 0 & 0 & 0 \\ 0 & -1 & 0 & 0 \\ 0 & 0 & 1 & 0 \end{pmatrix}$	–
$-x+\frac{1}{2},y+\frac{1}{2},-z+\frac{1}{2}$	$\begin{pmatrix} -1 & 0 & 0 & \frac{1}{2} \\ 0 & 1 & 0 & \frac{1}{2} \\ 0 & 0 & -1 & \frac{1}{2} \end{pmatrix}$	–
$x+\frac{1}{2},-y+\frac{1}{2},-z+\frac{1}{2}$	$\begin{pmatrix} 1 & 0 & 0 & \frac{1}{2} \\ 0 & -1 & 0 & \frac{1}{2} \\ 0 & 0 & -1 & \frac{1}{2} \end{pmatrix}$	$\begin{pmatrix} 1 & 0 & 0 & \frac{1}{2} \\ 0 & -1 & 0 & \frac{1}{2} \\ 0 & 0 & -1 & \frac{1}{2} \end{pmatrix}$
$-x,-y,-z$	$\begin{pmatrix} -1 & 0 & 0 & 0 \\ 0 & -1 & 0 & 0 \\ 0 & 0 & -1 & 0 \end{pmatrix}$	$\begin{pmatrix} -1 & 0 & 0 & 0 \\ 0 & -1 & 0 & 0 \\ 0 & 0 & -1 & 0 \end{pmatrix}$
$x,y,-z$	$\begin{pmatrix} 1 & 0 & 0 & 0 \\ 0 & 1 & 0 & 0 \\ 0 & 0 & -1 & 0 \end{pmatrix}$	–
$x+\frac{1}{2},-y+\frac{1}{2},z+\frac{1}{2}$	$\begin{pmatrix} 1 & 0 & 0 & \frac{1}{2} \\ 0 & -1 & 0 & \frac{1}{2} \\ 0 & 0 & 1 & \frac{1}{2} \end{pmatrix}$	–
$-x+\frac{1}{2},y+\frac{1}{2},z+\frac{1}{2}$	$\begin{pmatrix} -1 & 0 & 0 & \frac{1}{2} \\ 0 & 1 & 0 & \frac{1}{2} \\ 0 & 0 & 1 & \frac{1}{2} \end{pmatrix}$	$\begin{pmatrix} 1 & 0 & 0 & \frac{1}{2} \\ 0 & -1 & 0 & \frac{1}{2} \\ 0 & 0 & -1 & \frac{1}{2} \end{pmatrix}$

The structural relaxation results are summarized in Table III and Table IV corresponding to the Pnnm and Pbam space groups respectively. As mentioned previously, the experimental internal coordinates for BMT are from the room temperature X-ray results from Ref. 27 and they were also the starting positions for our LDA relaxation. We examined the shifts of the internal coordinates and noted the significant shifts as high as 0.5 angstrom observed at O atom in Pbam supercell. However, the overall larger displacement from the X-ray structure is observed in the Pnnm supercell in which the shifts for the ferroelectric active cations are 0.5 angstrom for Bi and 0.2 angstrom for Ti and Mg. The position of constituents atoms in BMT for Pbam and Pnnm from X-ray results and structural relaxation results are shown in Figure I, II, III and IV, respectively. The shifts of cations for both structures are different (details will be discussed in the later). The calculated total energies of the relaxed structures were 172.85 mRy and 212.44 mRy per formula unit lower than those of the x-ray structures for the Pnnm and Pbam supercells, respectively. The total energy of the relaxed Pbam supercell was also 47.09 mRy lower than that of Pnnm supercell. The force was reduced from 0.06 Ry/bohr (X-ray structure) to 0.001 Ry/bohr (calculated structure).

Results of the relaxation reduced the bondlength between Bi and the 12 fold oxygen nearest neighbors by 0.15 angstrom and between Ti/Mg and the 6 fold octahderal cage by 0.3 angstrom. It is interesting to note that the Ti-O and Mg-O bond distances are similar for both supercells for that Ti-O are shorter than Mg-O. The fact that MgO_6 octahedra are larger than TiO_6 is consistence with the ionic size difference of Ti and Mg cations (ionic radii are 0.61 angstrom and 0.72 angstrom for those of Ti and Mg respectively). The observation is consistent with the previous study by Miura et.al. [50]. The difference between the two supercells is more pronounced considering the nearest distance between Bi and B-cations. Bi in Pbam supercell favors the direction toward Ti causing 10% larger Bi-Mg bond distance than that of Bi-Ti. The Bi-B (Bi-Ti and Bi-Mg) distance are similar in Pnnm supercell. In other words, Bi redistributes the bondlength between Bi-Ti and Bi-Mg to have comparable Bi-Ti and Bi-Mg distance. Grinberg and coworkers [23] discussed the dependence of Bi-B cation repulsion on ionic size also found in the Pb oxide compound in which the smaller ionic size of B-cations would allow Bi to move closer toward B-cations. These are observed in our calculations as well. For Pbam, the nearest neighbor distance between Bi and Ti and Mg are 5.86 angstrom and 6.12 angstrom, and for Pnnm, they are 6.13 angstrom and 6.19 angstrom respectively. While the off-centering from the center of oxygen cages are 0.56 angstrom and 0.43 angstrom for Ti and Mg in Pbam and 0.53 angstrom and 0.33

angstrom for Ti and Mg in Pnnm. Taking into consideration of the fact that the ionic size of Ti is nearly 15 % smaller that of Mg, results of Pbam is of expected.

Figure II: Experimental structure of $Bi(Mg_{½}Ti_{½})O_3$ in Pbam supercell. The grey balls represents Bi cations while the small red balls are O, the cyan and pink denote Ti and Mg respectively.

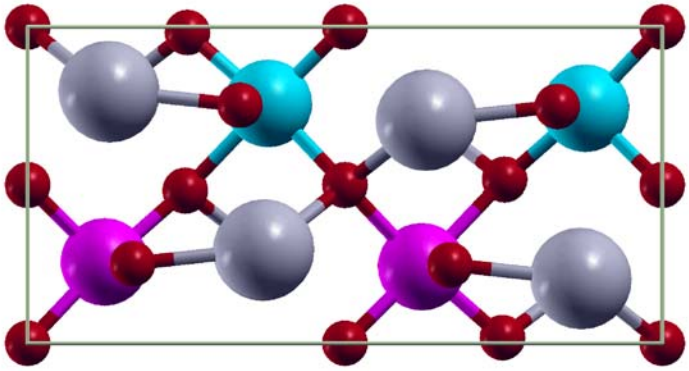

Figure III: Relaxed structure of $Bi(Mg_{½}Ti_{½})O_3$ in Pbam supercell. The grey balls represents Bi cations while the small red balls are O, the cyan and pink denote Ti and Mg respectively.

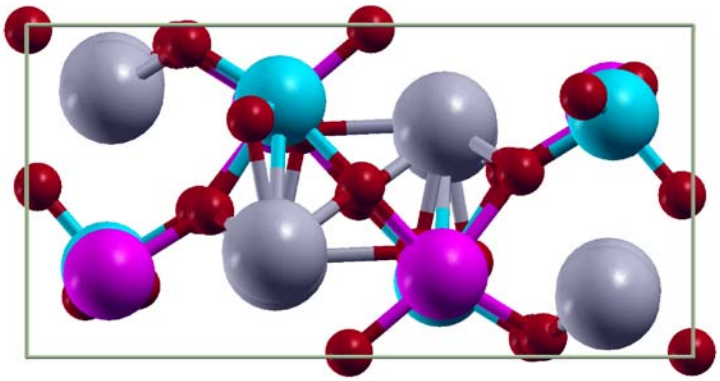

Figure IV: Experimental structure of $Bi(Mg_{½}Ti_{½})O_3$ in Pnnm supercell. The grey balls represents Bi cations while the small red balls are O, the cyan and pink denote Ti and Mg respectively.

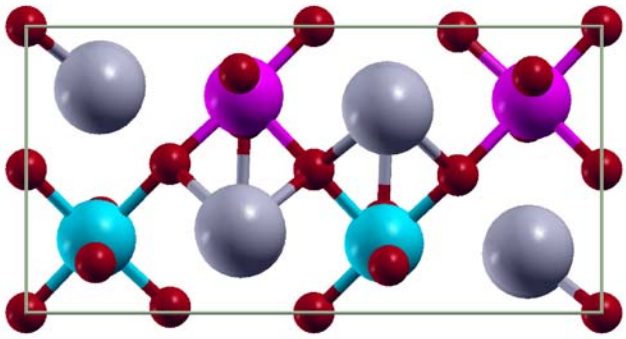

Figure V: Relaxed structure of $Bi(Mg_{½}Ti_{½})O_3$ in Pnnm supercell. The grey balls represents Bi cations while the small red balls are O, the cyan and pink denote Ti and Mg respectively.

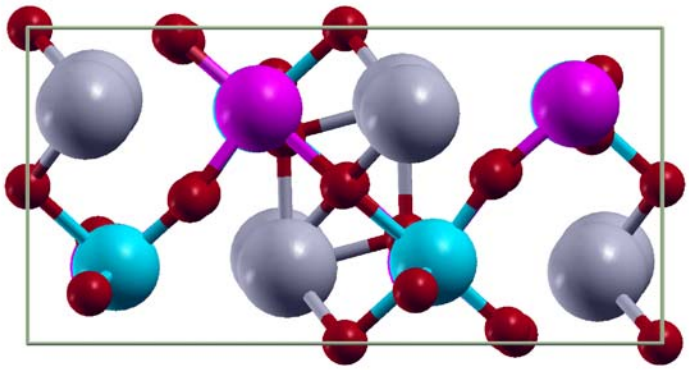

The qualitative behavior of the displacement of the cations, an analogy between the BMT and $PbZrO_3$ (PZ) can be drawn. The shifting pattern shows excellent agreement with the previously studied PZ crystal structure [41]. Comparing the Pbam relaxed supercell to the high symmetry supercell, the antiferroelectric active A-cations (Bi) displace antiparallel to the b-axis while the B-cations tend to displace less especially the Mg atoms. Similar to that of PZ, the direction of the Ti shifting was to compensate the gap due to the distortion of Bi. On the other hand the Pnnm

supercell, the antiferroelectric shifting is observed in the A-cations, Bi shift antiparallel to B-axis. Unlike the previously stated system where six of eight of Bi atoms surrounding B-cation move in the same direction leaving the other two in opposite direction, four Bi atoms in Pnnm supercells move alternately antiparallel with the other four and Mg/Ti displace toward Bi. The breathing motion of the octahedral have rather small changes from the X-ray results. The BO_6 tilting is observed around *a*-axis for Pnnm supercell and around *b*-axis for Pbam supercell causing the reduction in the length of *b* lattice parameter and in *a* lattice parameter in Pnnm and Pbam respectively as discussed in detail by Khalyavin. [27]

Table III: The LDA and room temperature experimental atomic positions in lattice coordinate for $Bi(Mg_{½}Ti_{½})O_3$ for Pnnm subgroup. The experimental values are from Ref. 27 and herein the same notation is used. The magnitude of displacement (ΔR) of calculated atomic positions from Experimental positions are given in angstrom.

Atom	Theory			Experiment			
	X	Y	Z	X	Y	Z	ΔR
Bi	0.5908	0.7603	0.5028	-0.3729	-0.2803	0.5000	0.47
Bi	0.1022	0.7728	0.5014	0.1289	0.7925	0.5000	0.32
Ti	0.6392	0.2583	0.7579	-0.3781	0.2425	0.7565	0.22
Mg	0.8641	0.7568	0.7437	0.8781	0.7425	0.7565	0.20
O	0.1110	0.3321	0.5142	0.1299	0.3352	0.5000	0.24
O	0.5972	0.3422	0.5091	0.6201	0.3249	0.5000	0.29
O	0.2559	0.4550	0.8020	0.2499	0.5197	0.8199	0.40
O	0.9966	0.0024	0.6903	0.0000	0.0000	0.6950	0.05
O	0.0000	0.4969	0.8025	0.0000	0.5000	0.8100	0.06
O	0.2317	0.9725	0.7088				

Table IV: The LDA and room temperature experimental atomic positions in lattice coordinate for $Bi(Mg_{½}Ti_{½})O_3$ for Pbam subgroup. The experimental values are from Ref. 27 and herein the same notation is used. The magnitude of displacement (ΔR) of calculated atomic positions from Experimental positions are given in angstrom.

Atom	Theory			Experiment			
	X	Y	Z	X	Y	Z	ΔR
Bi	0.6282	0.6787	0.0208	-0.3728	-0.2976	0.0000	0.21
Bi	0.1270	0.7981	0.4947	0.1293	0.7925	0.5000	0.06
Ti	0.3801	0.7701	0.7510	0.3789	0.7576	0.7481	0.08
Mg	0.6235	0.2506	0.7101	-0.3789	0.2424	0.7481	0.30
O	0.1644	0.2151	0.0090	0.1654	0.2519	0.0000	0.22
O	0.5882	0.3175	0.4915	0.5876	0.2458	0.5000	0.41
O	0.2754	0.4396	0.7238	0.2483	0.4824	0.6800	0.52
O	0.0020	0.9845	0.8088	0.0000	0.0000	0.8190	0.12
O	0.9837	0.4872	0.7677	0.0000	0.5000	0.8073	0.44
O	0.7411	0.5572	0.7042				

3.2 Pair distribution function

To further investigate the relaxed structure of BMT, we utilized the pair distribution function (PDF) analysis which is a method used to describe the distribution of the interatomic distance. PDF analysis can provide the information on all short-, medium-, and long-range ordering of the solid solutions. We calculated the pair distribution function by consider the density-density correlation of the interatomic distance of positions in BMT with the Gaussian broadening, that is we expressed the density-density correlation as

$$\rho_{ij}(r) = \frac{1}{\sqrt{2\pi\sigma^2}} \int e^{-|r_{ij}-r|^2/2\sigma^2} dr$$

with the broadening factor of 0.02.

Total pair distribution function of calculated and X-ray structure for up to 15 angstrom is shown in Figure V. Both supercells show substantial distortion from the experimental structures. In

addition, we examined the PDF for the constituent atoms, A-cation and B-cations as shown in Figure VI, VII, VIII for Bi, Mg and Ti respectively. We found that for Bi PDF, the Pbam supercell show more distortion as seen in the peak shape at 5 angstrom which is absent for the experimental structure. Even though the relaxed Pnnm Bi-PDF shows the noticeable distortion, closer similarities to the experimental structure are observed. In any case, both supercells share the common trend in the relaxation which shortens the bond distance between Bi and other atoms. The peaks for B-cations PDF show some similarity between both supercells that the Pbam supercell gives better agreement to the experiment structure than that of the Pnnm supercell. For Pbam supercell, shape and location of PDF peaks from the calculations resemble those of the X-ray results while for the Pnnm supercell, the relaxed PDF peaks indicate the arrangement aiming to the likeness between Mg and Ti PDF peaks which agree with the previous arguments.

Figure VI: Atomic pair distribution of relaxed BMT as a function of interatomic distance r (angstrom) for (a) Pbam and (b) Pnnm supercell.

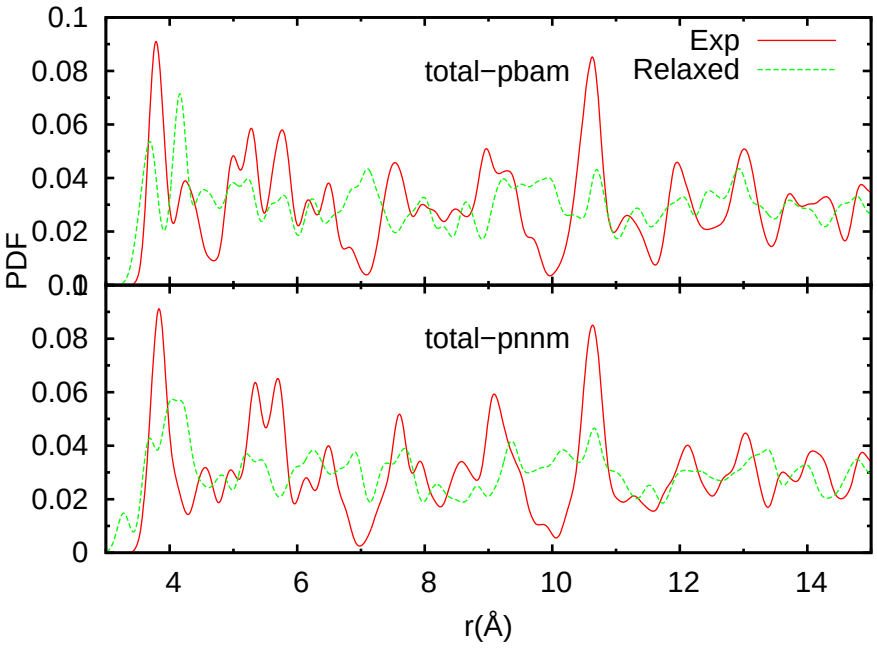

Figure VII: Bi pair distribution function as a function of interatomic distances r (angstrom) for (a) Pbam and (b) Pnnm subgroup.

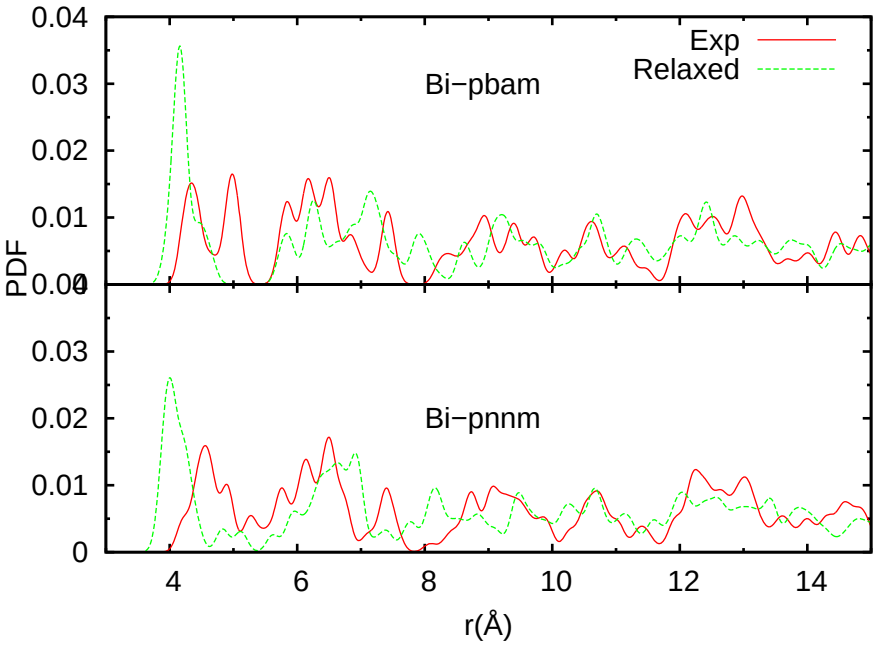

Figure VIII: Mg pair distribution function as a function of interatomic distances r (angstrom) for (a) Pbam and (b) Pnnm subgroup. }

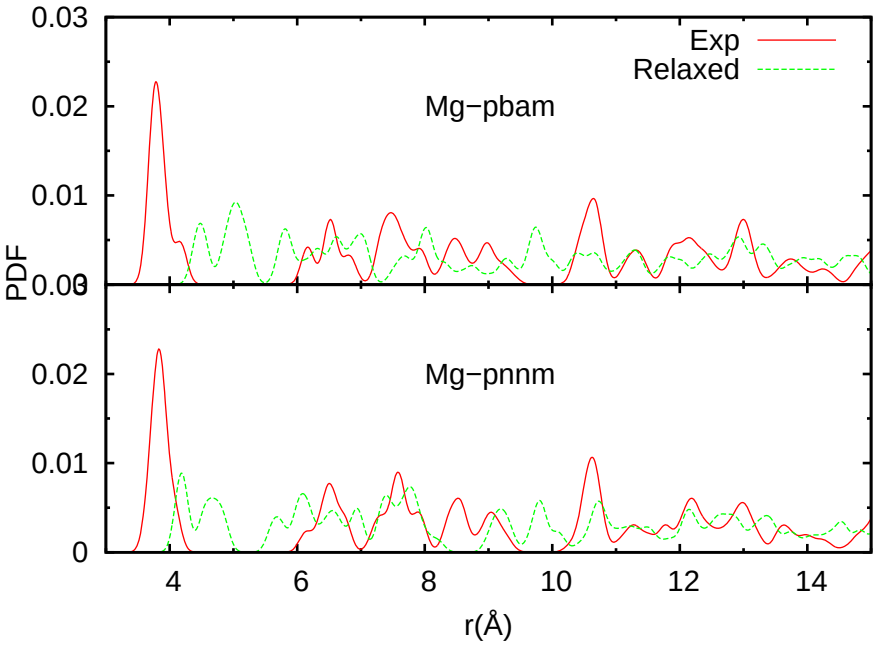

Figure IX: Ti pair distribution function as a function of interatomic distances r (angstrom) for (a) Pbam and (b) Pnnm subgroup**.**

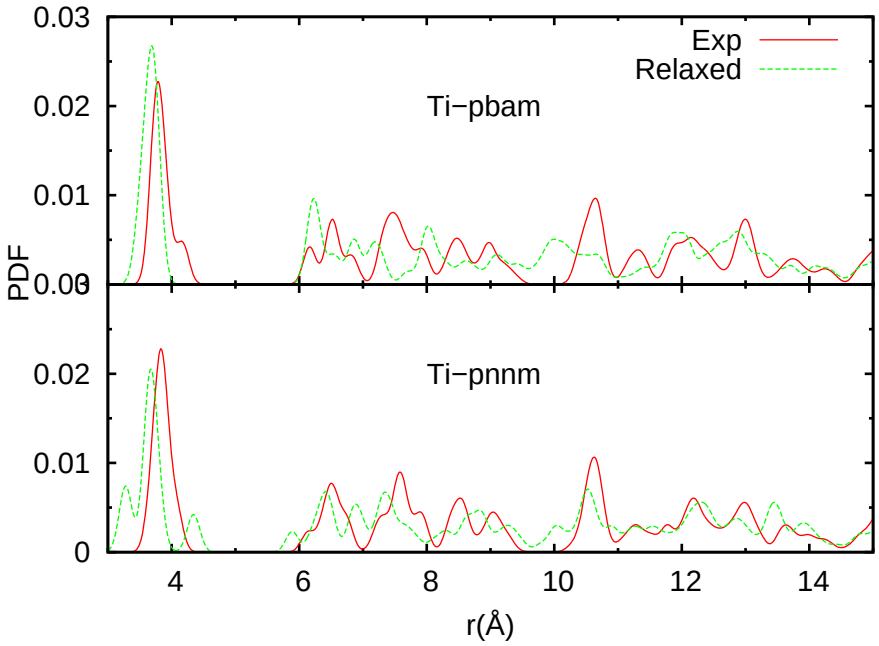

3.3 Electric field gradient

In a crystal, the electric field gradient (EFG) depends only on the nuclear positions and the electronic charge density therefore the values of EFG at an atomic nucleus are obtained from the non-spherical field of the electrons and other ions. EFG can be used to understand the non-spherical feature of cations e.g. the local displacement. We calculated the EFG for all atoms in the supercells. Table V and Table VI show the EFG for all atoms of BMT in Pbam and Pnnm respectively. The similarity of the values of the EFG for both supercells are observed with the exception on the EFG at Bi(Bi(1) and Bi(2)). For that the EFG at Bi in BMT of the Pbam are large and comparable in magnitude but the substantial difference in values of EFG at the two Bi are noted for the Pnnm supercell.

Table V: Calculated EFGs (V_{zz} in units of 10^{21} V/m^2) for BMT with imposed Pbam subgroup

Atom	EFG (10^{21})	η
Bi	17.05	0.25
Bi	24.55	0.41
Ti	1.99	0.39
Mg	0.73	0.61
O	-4.13	0.13

O	-3.00	0.30
O	-3.28	0.52
O	-0.69	0.98
O	-0.89	0.07
O	-2.47	0.39

Table VI: Calculated EFGs (V_{zz} in units of 10^{21} V/m^2) for BMT with imposed Pbam subgroup

Atom	EFG (10^{21})	η
Bi	34.94	0.99
Bi	-8.34	0.53
Ti	-1.88	0.07
Mg	-0.59	0.21
O	-0.95	0.82
O	-2.47	0.29
O	-3.77	0.69
O	1.39	0.16
O	-1.12	0.73
O	-0.91	0.23

Chapter 4: Summary

To summarize, we report a first-principles structural study of $Bi(Mg_{½}Ti_{½})O_3$. The comparison between the relaxed structures and the X-ray refinement structures of the two supercells, Pbam and Pnnm were made. We optimized the atomic position by using the experimental structures as our starting position. The relaxed structures (both supercells) were further analyzed by plotting the pair distribution function for BMT and each constituent atoms as well as calculating the electric field gradients. The atomic position after relaxation procedure showed the displacement of 0.5 angstrom for O in Pbam supercell but the overall larger displacement from the X-ray structure is observed in the Pnnm supercell in which the shifts for the ferroelectric active cations are 0.5 angstrom for Bi and 0.2 angstrom for Ti and Mg. The BMT structures after relaxation show the lowering in energy of 172.85 mRy and 212.44 mRy per formula unit than those of X-ray structure for Pnnm and Pbam sueprcells, respectively. Wih the Pbam total energy is 47.09 mRy lower than that of Pnnm supercell. The root mean square (rms) force has reduced from 0.06 Ry/bohr (X-ray structure) to 0.001 Ry/bohr (calculated structure).
Despite the similarity in XRD patterns between these two supercells, the LDA calculations revealed the difference in A-cations distortion and the octahedral tilting between Pnnm and Pbam supercells. In addition, the pair distribution function shows noticeable distortion from experimental structures. Both structures displaced in the direction to shorten the bond distance between Bi and other atoms. The electric field gradient support the fact that B-cations (Ti and Mg) are more rigid than Bi.

Bibliography

[1] B. Noheda, D. E. Cox, G. Shirane, J. A. Gonzalo, L. E. Cross, and S. E. Park, *Appl. Phys. Lett.,* **74**, 2059 (1999).

[2] I. Grinberg, M. R. Suchomel, P. K. Davies and A. M. Rappe. *J. of Appl. Phys.* **98**, 094111 (2005).

[3] M. R. Suchomel and P. K. Davies. *J. of Appl. Phys.* **96**, 4405 (2004).

[4] R. E. Cohen, *Nature*, **358**, 136 (1992).

[5] L. Bellaiche, A. Garcia, and D. Vanderbilt, *Phys. Rev. Lett*., **84**, 5427 (2000).

[6] H. Fu and R. E. Cohen, *Nature*, 403, 281 (2000).

[7] P. Ghosez, E. Cockayne, U. V. Wanghmare, and K. M. Rabe, *Phys. Rev. B*, **60**, 836 (1999).

[8] G. Saghi-Szabo, R. E. Cohen, and H. Krakauer, *Phys. Rev. B*, **59**, 12771 (1999).

[9] M. Fornari and D. J. Singh, *Phys. Rev. B*, **63**, 092101 (2001).

[10] G. A. Samara, J. Phys.:Condens. Matter, **15**, R367 (2003).

[11] Z. Yu, R. Guo, and A. S. Bhalla, *Appl. Phys. Lett*., **77**, 1535 (2000).

[12] J. Kreisel, P. Bouvier, M. Maglione, B. Dkhil, and A. Simon, *Phys. Rev. B*, **69**, 092104 (2004).

[13] Y. Saito, H. Takao, T. Tani, T. Nonoyama, K. Takatory, T. Homma, T. Nagaya, and M. Nakamura, *Nature*, **432**, 84 (2004).

[14] Y. Guo, K. Kakimoto, and H. Ohsato, *Appl. Phys. Lett*., **85**, 4121 (2004).

[15] E. Ringgaard and T. Wurlitzer, *J. Eur. Ceram. Soc*., **25**, 2701 (2005).

[16] M. Suewattana and D. J. Singh, *Phys. Rev. B*, **82**, 014114 (2010).

[17] S. Ke, H. Huang, S. Yu, and L. Zhou, *J. Appl. Phys*, **107**, 084112 (2010).

[18] C. Laulhe, F. Hippert, R. Bellissent, A. Simon, and G. J. Cuello, *Phys. Rev. B*, **79**, 064104 (2009).

[19] T. Maiti, R. Guo, and A. S. Bhalla, *J. AM. Ceram. Soc*., **91**, 1769 (2008).

[20] S. Wada, K. Yamato, P. Pulpan, N. Kumada, B. Lee, T. Iijima, C. Moriyoshi, and Y. Kuroiwa, *J. Appl. Phys*., **108**, 094114 (2010).

[21] R. E. Eitel, S. J. Zhang, T. R. Shrout, C. A. Randall, and I. Levin, *J. Appl. Phys*., **96**, 2828 (2004).

[22] R. E. Eitel, C. A. Randall, T. R. Shrout, P. W. Rehrig, W. Hackenberger, and S.-E. Park, *Jpn. J. Appl. Phys.*, **40**, 5999 (2001).

[23] I. Grinberg and A. M. Rappe, *Phys. Rev. Lett*., **98**, 037603 (2007).

[24] S. Takagi, A. Subedi, D. J. Singh, and V. R. Cooper, *Phys. Rev. B*, **81**, 134106 (2010).

[25] S. Takagi, A. Subedi, V. R. Cooper, and D. J. Singh, *Phys. Rev. B*, **82**, 134108 (2010).

[26] M. R. Suchomel, A. W. Fogg, M. Allix, H. Niu, J. B. Claridge, and M. J. Rosseinsky, *Chem. Mater.*, **18**, 798 (2006).

[27] D. D. Khalyavin, A. N. Salak, N. P. Vyshatko, A. B. Lopes, N. M. Olekhnovich, A. V. Pushkarev, I. I. Morez, and Y. V. Radyush, *Chem. Mater*., **18**, 5104 (2006).

[28] A. A. Belik, S. Iikubo, K. Kodama, N. Igawa, S. Shamoto, S. Niitaka, M. Azuma, Y. Shimakawa, M. Takano, F. Izumi, and E. Takayama-Muromachi, *Chem. Mater*., **18**, 798 (2006).

[29] T. Sebastian, I Sterianou, D. C. Sinclair, A. J. Bell, D. A. Hall, and I. M. Reaney, J. Electroceram, 25, 130 (2010).

[30] J. Chen, X. Tan, W. Jo, and J. Rodel, J. Appl. Phys., 106, 034109 (2009).

[31] S. Sharma and D. A. Hall, J. Mater Sci: Mater Electron, 21, 405 (2010).

[32] Q. Zhang, Z. Li, F. Li, Z. Xu, and X. Yao, J. Am. Ceram. SOc., 93, 3330 (2010).

[33] P. Hu, J. Chen, X. Sun, J. Deng, X. Chen, R. Yu, L. Qiao, and X. Xing, J. Mat. Chem., 19, 1648 (2009).

[34] R. Rai, A. Sinha, S. Sharmac, and N. Sinha, *J. Alloys Compd*., **486**, 273 (2009).

[35] A. Moure, M. Alguero, L. Pardo, E. Ringgaard, and A. F. Pedersen, *J. Eur. Ceram. Soc*., **27**, 237 (2007).

[36] M. D. Snel, W. A. Groen, ad G. D. With, *J. Eur. Ceram. Soc*., **25**, 3229 (2005).

[37] C. A. Randall, R. Eitel, B. Jones, T. R. Shrout, D. I Woodward, and I. M. Reaney, *J. of Appl. Phys.*, **95**, 3633 (2004).

[38] A. V. Pushkarev, N. M. Olekhnovich, and Y. V. Radyish*, Inorganic Materials*, **45**, 1062 (2009).

[39] C. A. Randall, R. Eitel, B. Jones, T. R. Shrout, D. I. Woodward, and I. M. Reaney, *J. of Appl. Phys.*, **95**, 3633 (2004).

[40] F. Jona, G. SHirane, F. Mazzi, and R. Pepinsky, *Phys. Rev*., **105**, 849 (1957).

[41] M. D. Johannes and D. J. Singh, *Phys. Rev. B*, **71**, 212101 (2005).

[42] J. A. Rodriguea, A. Etxeberria, L. Gonzalez, and A. Maiti, *J. of Chem. Phys*., **117**, 2699 (2002).

[43] D. J. Singh, *Phys. Rev. B*, **52**, 12559 (1995).

[44] I. Grinberg, V. R. Cooper, and A. M. Rappe, *Nature*, **419**, 909 (2002).

[45] D. I. Bilc and D. J. Singh, *Phys. Rev. Lett*., **96**, 147602 (2006).

[46] D. J. Singh and L. Nordstrom, eds., Planewaves, Pseudopotentials and the LAPW method (Kluwer Academic, Boston, 1994).

[47] P. Hohenberg and W. Kohn*, Phys. Rev*., **136** (3B) B864-B871 (1964).

[48] R. O. Jones and O. Gunnarsson, *Rev. Mod. Phys*. **61**, 689 (1989).

[49] W. Kohn and L. J. Sham, *Phys. Rev*., **140** (4A): A1133-A1138 (1965).

[50] K. Miura, M. Kubota, M. Azuma, and H. Funakubo, *Jap. J. of Appl. Phys*., **48**, 09KF05 (2009).

[51] I. Grinberg, M. R. Schomel, P. K. Davies, and A. M. Rappe, *J. Appl. Phys*., **98**, 094111 (2005).

Output จากโครงการวิจัยที่ได้รับทุนจาก สกอ. และ สกว.

1. ผลงานตีพิมพ์ในวารสารวิชาการนานาชาติ

   M. Suewattana, D. J. Singh, S. Limpijumnong, "*Crystal structure study of Bi($Mg_{\square}Ti_{1/2}$)O_3 by density functional theory*", in preparation to be submitted to Physical Review B.

2. การนำผลงานวิจัยไปใช้ประโยชน์

   - เชิงวิชาการ: มีการพัฒนาการจัดตั้งคลัสเตอร์คอมพิวเตอร์ขนาดเล็ก ทำให้เกิดการฝึกหัดและพัฒนาความเชี่ยวชาญสำหรับนักศึกษาและอาจารย์

3. อื่นๆ

   - เสนอผลงานแบบโปสเตอร์ ที่การประชุมนานาชาติ European Meeting on Ferroelectricity ณ เมือง Bordeaux ประเทศสาธารณรัฐฝรั่งเศส ระหว่างวันที่ 26 มิถุนายน – 2 กรกฎาคม 2554